Low-Complexity Adaptive Multisine Waveform Design for Wireless Power Transfer

Bruno Clerckx and Ekaterina Bayguzina

***Abstract*—Channel-adaptive waveforms for wireless power transfer significantly boost the dc power level at the rectifier output. However, the design of those waveforms is computationally complex and does not lend itself easily to practical implementation. We here propose a low-complexity channel-adaptive waveform design whose performance is very close to that of the optimal design. Performance evaluations confirm the advantages of the new design in various rectifier topologies, with gains in dc output power of 100% over conventional waveforms.**

***Index Terms*—Rectenna, waveform, wireless power transfer (WPT).**

I. Introduction

WIRELESS power transfer (WPT) via radio-frequency radiation is nowadays attracting much attention, with clear applications in wireless sensor networks and Internet of things [1]. The major challenge facing far-field wireless power designers is to find ways to enhance the end-to-end power transfer efficiency, or equivalently increase the dc power level at the output of the rectenna without increasing the transmit power, and for devices located tens to hundreds of meters away from the transmitter. To that end, the vast majority of the technical efforts in the literature has been devoted to the design of efficient rectennas, *a.o.* [1], so as to increase the RF-to-dc conversion efficiency.

Another promising approach is to design efficient WPT signals (including waveforms, beamforming, and power allocation) [2], [3]. Indeed, the transmit signal design has a major impact on the end-to-end power transfer efficiency as it influences the signal strength at the input of the rectenna, but also the RF-to-dc conversion efficiency due to the rectifier nonlinearity. Traditional approaches consist in using waveforms that exhibit high peak-to-average power ratio (PAPR) [4]–[7]. Unfortunately, those approaches were heuristic and ignored the presence of the time-varying wireless propagation channel that is subject to multipath and fading. Multipath has for consequence that the transmit and the received (at the input of the rectenna) waveforms are completely different. Hence, the transmit waveforms should be designed in accordance with the channel status. However, all those approaches in the RF literature [4]–[7] are based on an open-loop architecture with waveforms being static. A systematic design and optimization of channel-adaptive waveform and signal for WPT has recently been tackled in [3] and [8] and further extended in [9] for large-scale WPT. Gains over various baseline waveforms have been shown to be very significant. This adaptive design leads to a closed-loop architecture where the channel state information is acquired to the transmitter and the transmit signal is dynamically adapted so as to maximize the dc power at the output of the rectifier, accounting for the wireless channel and the rectifier nonlinearity. Contrary to what is claimed in [4]–[7], maximizing PAPR was shown in [3] not to be a right approach to design efficient WPT signal. High PAPR signals are useful if the channel is frequency flat, not in the presence of multipath and frequency selectivity.

Unfortunately, those optimized and adaptive waveforms do not lend themselves easily to practical implementation because they result from a nonconvex optimization problem that would require to be solved real-time as a function of the channel state information (CSI). This is computationally intensive. Those waveforms can therefore be viewed as benchmarks we should aim for performance-wise. What we propose in this letter is a design of multisine waveform, adaptive to CSI, whose performance is very close to the optimal design of [3] and [8] but whose complexity is significantly lower. Indeed, the proposed design results from a simple scaled matched filter that has the effect of allocating more (resp. less) power to the frequency components corresponding to large (resp. weak) channel gains.

Notations: Bold letters stand for vectors or matrices. $|.|$ and $\|.\|$ refer to the absolute value of a scalar and the 2-norm of a vector. $\mathcal{E}\{.\}$ refers to the averaging operator.

II. WPT System Model

A. Transmit and Received Signal

Consider a multisine signal $x(t) = \Re\{\sum_{n=0}^{N-1} w_n e^{j2\pi f_n t}\}$ (with N sinewaves) transmitted at time t over a single antenna with $w_n = s_n e^{j\phi_n}$, where s_n and ϕ_n refer to the amplitude and phase of the nth sinewave at frequency f_n, respectively. We assume that the frequencies are evenly spaced, i.e., $f_n = f_0 + n\Delta_f$ with Δ_f the frequency spacing. The magnitudes and phases of the sinewaves are collected into vectors $\mathbf{s}$ and $\mathbf{\Phi}$, whose nth entry writes as s_n and ϕ_n, respectively. The transmit power constraint is given by $\mathcal{E}\{|x|^2\} = \frac{1}{2}\|\mathbf{s}\|^2 \leq P$.

The transmitted sinewaves propagate through a multipath channel, characterized by L paths whose delay, amplitude, and phase are respectively denoted as τ_l, α_l, ξ_l, $l = 1, \ldots, L$. The signal received at the single-antenna receiver is written as

$$y(t) = \sum_{n=0}^{N-1} s_n A_n \cos(\varpi_n t + \psi_n) = \Re\left\{\sum_{n=0}^{N-1} h_n w_n e^{j\varpi_n t}\right\} \quad (1)$$

Manuscript received April 18, 2017; revised May 9, 2017; accepted May 17, 2017. Date of publication May 23, 2017; date of current version August 7, 2017. This work was supported by the Engineering and Physical Sciences Research Council under Grant EP/K502856/1, Grant EP/L504786/1, and Grant EP/P003885/1. *(Corresponding author: Bruno Clerckx.)*

The authors are with the Imperial College London, London SW7 2AZ, U.K. (e-mail: b.clerckx@imperial.ac.uk; ekaterina.bayguzina08@imperial.ac.uk).

Color versions of one or more of the figures in this letter are available online at http://ieeexplore.ieee.org.

Digital Object Identifier 10.1109/LAWP.2017.2706944

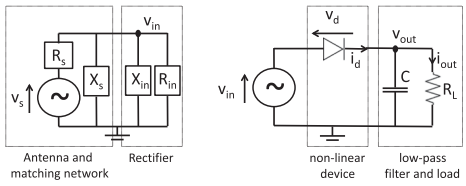

Fig. 1. Antenna equivalent circuit (left) and a single diode rectifier (right).

where $h_n = A_n e^{j\bar{\psi}_n} = \sum_{l=0}^{L-1} \alpha_l e^{j(-2\pi f_n \tau_l + \xi_l)}$ is the channel frequency response at frequency f_n and $\varpi_n = 2\pi f_n$. A_n and ψ_n are defined such that $A_n e^{j\psi_n} = A_n e^{j\left(\phi_n + \bar{\psi}_n\right)} = e^{j\phi_n} h_n$.

B. Antenna Equivalent Circuit Model

The antenna model reflects the power transfer from the antenna to the rectifier through the matching network. As illustrated in Fig. 1 (left), a lossless antenna combined with a matching network is modeled as a voltage source $v_{\rm s}(t)$ followed by a series resistance $R_{\rm s}$ and a parallel reactance $X_{\rm s}$. The rectifier is modeled as a resistance $R_{\rm in}$ in parallel with a reactance $X_{\rm in}$. Assuming perfect matching ($R_{\rm in} = R_{\rm s}$, $X_{\rm in} = -X_{\rm s}$), all the available RF power $P_{\rm in,av}$ is transferred to the rectifier and absorbed by $R_{\rm in}$, so that $P_{\rm in,av} = \mathcal{E}\left\{ |v_{\rm in}(t)|^2 \right\}/R_{\rm s}$. Since $P_{\rm in,av} = \mathcal{E}\left\{ |y(t)|^2 \right\}$, $v_{\rm in}(t) = y(t)\sqrt{R_{\rm s}}$.

C. Rectifier and Diode Nonlinear Model

Consider a rectifier composed of a single series diode followed by a low-pass filter with load as in Fig. 1 (right). Denoting the voltage drop across the diode as $v_{\rm d}(t) = v_{\rm in}(t) - v_{\rm out}(t)$, where $v_{\rm in}(t)$ is the input voltage to the diode and $v_{\rm out}(t)$ is the output voltage across the load resistor, a tractable behavioral diode model is obtained by Taylor series expansion of the diode characteristic equation $i_{\rm d}(t) = i_{\rm s}\left(e^{\frac{v_{\rm d}(t)}{n v_{\rm t}}} - 1\right)$ (with $i_{\rm s}$ the reverse bias saturation current, $v_{\rm t}$ the thermal voltage, and n the ideality factor assumed equal to 1.05) around a quiescent operating point $v_{\rm d} = a$, namely $i_{\rm d}(t) = \sum_{i=0}^{\infty} k_i' \left(v_{\rm d}(t) - a\right)^i$, where $k_0' = i_{\rm s}\left(e^{\frac{a}{n v_{\rm t}}} - 1\right)$ and $k_i' = i_{\rm s} \frac{e^{\frac{a}{n v_{\rm t}}}}{i!(n v_{\rm t})^i}$, $i = 1, \ldots, \infty$. Assume a steady-state response and an ideal low-pass filter such that $v_{\rm out}(t)$ is at constant dc level. Choosing $a = \mathcal{E}\left\{v_{\rm d}(t)\right\} = -v_{\rm out}$, we can write $i_{\rm d}(t) = \sum_{i=0}^{\infty} k_i' v_{\rm in}(t)^i = \sum_{i=0}^{\infty} k_i' R_{\rm s}^{i/2} y(t)^i$. Truncating the expansion to order 4, the dc component of $i_{\rm d}(t)$ is the time average of the diode current, and is obtained as $i_{\rm out} \approx k_0' + k_2' R_{\rm s} \mathcal{E}\left\{y(t)^2\right\} + k_4' R_{\rm s}^2 \mathcal{E}\left\{y(t)^4\right\}$.

III. Low-Complexity Adaptive Waveform Design

Assuming the CSI (in the form of frequency response h_n) is known to the transmitter,[1] we aim at finding the set of amplitudes and phases $\mathbf{s}, \mathbf{\Phi}$ that maximizes $i_{\rm out}$. Following [3], this is equivalent to maximizing the quantity

$$z_{\rm dc}\left(\mathbf{s}, \mathbf{\Phi}\right) = k_2 R_{\rm s} \mathcal{E}\left\{y(t)^2\right\} + k_4 R_{\rm s}^2 \mathcal{E}\left\{y(t)^4\right\} \tag{2}$$

where $k_i = \frac{i_s}{i!(n v_{\rm t})^i}$, $i = 2, 4$. Assuming $i_{\rm s} = 5\ \mu A$, a diode ideality factor $n = 1.05$ and $v_{\rm t} = 25.86\,{\rm mV}$, typical values are given by $k_2 = 0.0034$ and $k_4 = 0.3829$.

The waveform design problem can therefore be written as

$$\max_{\mathbf{s}, \mathbf{\Phi}} z_{\rm dc}(\mathbf{s}, \mathbf{\Phi}) \text{subject to } \|\mathbf{s}\|^2 \leq 2P \tag{3}$$

where $z_{\rm dc}$ is given in (4) shown at the bottom of this page, after plugging $y(t)$ of (1) into (2).

From [3] and [8], the optimal phases are given by $\phi_n^\star = -\bar{\psi}_n$, while the optimum amplitudes result from a nonconvex posynomial maximization problem that can be recast as a reversed geometric program (GP) and solved iteratively but does not easily lend itself to practical implementation. Indeed, according to [10], reversed GP takes exponential time to compute an optimal solution. Interestingly, as noted in [3], the optimized waveform has a tendency to allocate more power to frequencies exhibiting larger channel gains. Motivated by this observation, we propose here, as a suboptimal solution to (3), a simple, closed-form, and low-complexity strategy, denoted as scaled matched filter (SMF), which selects the phases as $\phi_n^\star$ but chooses the amplitudes of sinewaves according to[2]

$$s_n = c A_n^\beta \tag{5}$$

where c is the constant satisfying the transmit power constraint $\frac{1}{2}\sum_{n=0}^{N-1} s_n^2 = P$ and $\beta \geq 1$. The complex weight of the SMF waveform on frequency n is finally given in closed form as

$$w_n = e^{-j\bar{\psi}_n} A_n^\beta \sqrt{\frac{2P}{\sum_{n=0}^{N-1} A_n^{2\beta}}}. \tag{6}$$

The SMF waveform design is only a function of a single parameter, namely β. By taking $\beta = 1$, we get a matched filter-like behavior, where the amplitude of sinewave n is linearly proportional to A_n. This is reminiscent of maximum ratio transmission in communication. On the other hand, by scaling A_n using an exponent $\beta > 1$, we further amplify the strong frequency components and attenuate the weak ones.

β can either be optimized on a channel basis or be fixed once for all. Plugging (6) into (4), we get (7) shown at the bottom of this page. For a given channel realization, the best β can be obtained as the solution of the unconstrained optimization problem $\beta^\star = \arg\max_\beta z_{\rm dc,SMF}$, which can be solved numerically using Newton's method.

[1] Inspired by communication systems, we could envision a pilot transmission phase (on the uplink) and a channel estimator at the power base station. Alternatively, approaches relying on CSI feedback could be exploited [2].

[2] Note that, following [3], the SMF strategy is easily extendable to multiple transmit antennas by replacing A_n with the norm of the vector channel.

$$z_{\rm dc}(\mathbf{s}, \mathbf{\Phi}) = \frac{k_2}{2} R_{\rm s} \left[\sum_{n=0}^{N-1} s_n^2 A_n^2\right] + \frac{3k_4}{8} R_{\rm s}^2 \left[\sum_{\substack{n_0, n_1, n_2, n_3 \\ n_0 + n_1 = n_2 + n_3}} \left[\prod_{j=0}^{3} s_{n_j} A_{n_j}\right] \cos(\psi_{n_0} + \psi_{n_1} - \psi_{n_2} - \psi_{n_3})\right]. \tag{4}$$

$$z_{\rm dc,SMF} = k_2 R_{\rm s} P \left[\sum_{n=0}^{N-1} \frac{A_n^{2(\beta+1)}}{\sum_{n=0}^{N-1} A_n^{2\beta}}\right] + \frac{3k_4}{2} k_4 R_{\rm s}^2 P^2 \left[\sum_{\substack{n_0, n_1, n_2, n_3 \\ n_0 + n_1 = n_2 + n_3}} \frac{\prod_{j=0}^{3} A_{n_j}^{\beta+1}}{\left[\sum_{n=0}^{N-1} A_n^{2\beta}\right]^2}\right]. \tag{7}$$

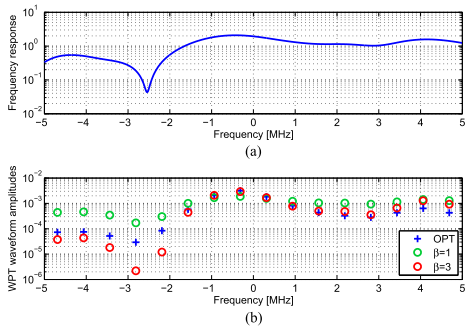

Fig. 2. (a) Frequency response of the wireless channel and (b) WPT waveform magnitudes ($N = 16$) for 10-MHz bandwidth.

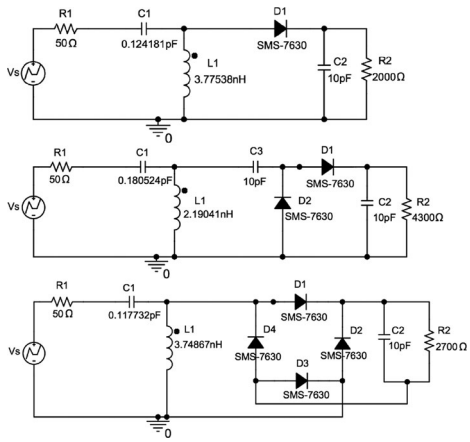

Fig. 3. Single series, voltage doubler, and diode bridge rectifiers.

In order to get some insights into the SMF strategy (5), we consider a frequency-selective channel whose frequency response is given by Fig. 2(a), a transmit power of -20 dBm, $N = 16$ sinewaves centered around 5.18 GHz with a frequency gap fixed as $\Delta_f = B/N$ and $B = 10$ MHz. Assuming such a channel realization, we compare in Fig. 2(b) the magnitudes of the SMF waveform (with $\beta = 1, 3$) and of the optimum (OPT) waveform obtained using the reversed GP algorithm derived in [3] and [8]. The OPT waveform has a tendency to allocate more power to frequencies exhibiting larger channel gains. Choosing $\beta = 1$ would allocate power proportionally to the channel strength but has a tendency to underestimate the power to be allocated to strong channels and overestimate the power to be allocated to weak channels. On the other hand, suitably choosing $\beta > 1$ better emphasizes the strong channels and deemphasizes the weak channels.

IV. Performance Evaluations

In this section, we evaluate through simulations the performance of the waveforms using the rectifier configurations of Fig. 3. We consider a point-to-point scenario representative of a WiFi deployment at a center frequency of 5.18 GHz with a 36-dBm transmit power, isotropic transmit antennas, 2 dBi receive antenna gain, and 58 dB path loss in a large open-space environment with a non-line-of-sight channel power-delay profile obtained from model B [11]. Taps are modeled as independent identically distributed (i.i.d.) circularly symmetric complex Gaussian random variables and normalized such that the average received power is -20 dBm. The N sinewaves are centered around 5.18 GHz with $\Delta_f = B/N$ and $B = 10$ MHz.

The rectennas in Fig. 3 are optimized for a multisine input signal composed of four in-phase sinewaves with uniform power allocation and the available RF power of -20 dBm. This is motivated by the fact that due to the channel frequency selectivity, out of a large number of sinewaves, only a few are allocated significant power [e.g., as in Fig. 2(b)]. The package parasitics of components are ignored in all simulator models. The L-matching network is optimized together with the load resistance with the objective to maximize the output dc power and minimize impedance mismatch due to a signal of varying instantaneous power using an ADS Harmonic Balance with five harmonics, and then optimization is run with ADS Transient to further improve efficiency. It is found that the peak reverse voltage (1.3 V) for all simulated N (≤ 32) is lower than the diode breakdown voltage (2 V for SMS7630). The diode junction capacitance ($C_{j0} = 0.14$ pF) is included in the circuit simulations (though it is omitted in Section II-C because it introduces negligible losses to the output dc power in the frequency range of interest and at low input power levels).

In Fig. 4(a), we display $z_{\rm dc}$ (assuming $R_s = 50\,\Omega$) averaged over several hundreds channel realizations for various waveforms. The traditional fixed waveform is not adaptive to CSI and is obtained by allocating power uniformly (UP) across sinewaves and fixing the phases ϕ_n as 0 [4]–[6]. Adaptive matched filter (MF) is a particular case of the proposed SMF with $\beta = 1$. SMF with $\beta^\star$ refers to the SMF waveform where β is optimized on each channel realization using Newton's method. Adaptive OPT is the optimal strategy resulting from the reversed GP derived in [3] and [8]. The proposed strategy SMF with $\beta = 3$ comes very close to the optimal performance but incurs a significantly lower complexity since the weights are given in closed form.

In Fig. 4(b)–(d), we evaluate the waveform performance using PSpice simulations. To that end, the waveforms after the wireless channel have been used as inputs to the rectennas of Fig. 3, and the dc power delivered to the load has been observed. The average dc power, where averaging is done over many realizations of the wireless channel, is displayed in Fig. 4(b)–(d) as a function of N. We confirm the observations made using the $z_{\rm dc}$ metric in Fig. 4(a), namely that the performance of SMF with $\beta = 3$ or $\beta^\star$ is very close to that of OPT despite the much lower design complexity. The PSpice evaluations also confirm the benefits of the SMF and OPT waveforms over the conventional nonadaptive UP multisine waveform and the usefulness of the waveform design methodology of [3] in a wide range of rectifier configurations. Results also highlight the importance of efficient waveform design for WPT. Taking for instance Fig. 4(b), we note that the RF-to-dc conversion efficiency jumps from less than 20% to over 60% by making use of 32 sinewaves rather than a single sinewave. We also note that at low average input power, a single series rectifier is preferable over the voltage doubler or diode bridge, which is in line with observations made in [5].

Results also highlight that the nonlinear rectifier model and the waveform design and optimization are valid for the multiple-diode rectenna configurations. This is because only a subset of diodes are conducting during a half-cycle of the input waveform and such operating point a can be found so that $z_{\rm dc}$ can still be expressed as in (2). In case of the voltage doubler, ignoring the voltage gain due to the matching network and the forward voltage drops across the diodes, the capacitor C_3 is charged to the peak of the input waveform $\hat{v}_{\rm in}$ during the negative half-cycle. During the positive half-cycle, the voltage across the diode D_1 can be obtained as $v_{\rm d1}(t) \approx v_{\rm in}(t) + \hat{v}_{\rm in} - v_{\rm out}(t)$, so the appropriate choice of the operating point is $a = \hat{v}_{\rm in} - v_{\rm out}$.

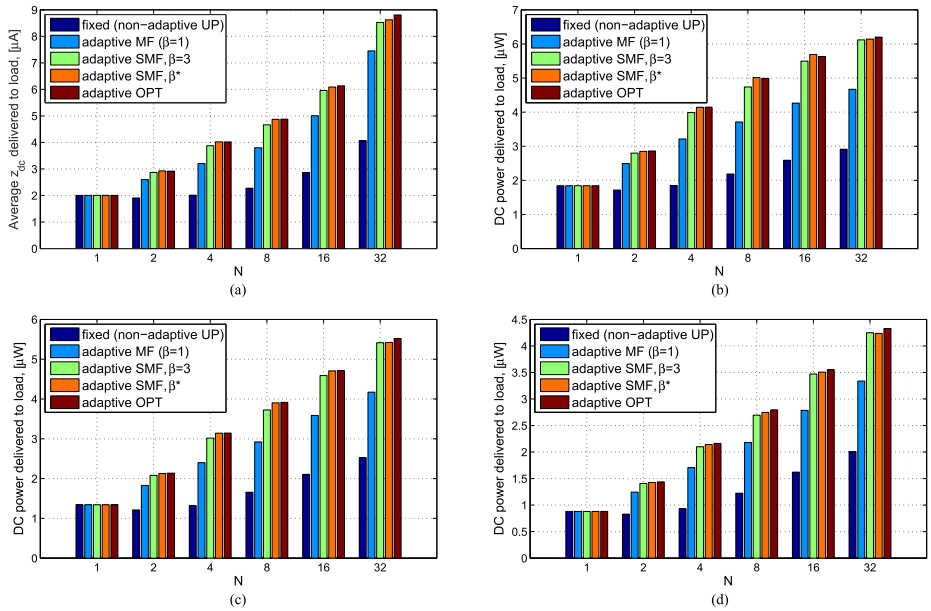

Fig. 4. Average z_{dc} and average dc power delivered to the load as a function of N for various rectifiers. (a) Average z_{dc}, (b) single series, (c) voltage doubler, and (d) diode bridge.

In case of the diode bridge, when the diodes D_1 and D_3 are conducting during the positive half-cycle, the current flowing through and the voltage across the diodes D_1 and D_3 is equal, so $v_{\mathrm{d1}}(t) = v_{\mathrm{in}}(t) - v_{\mathrm{out}}(t) - v_{\mathrm{d3}}(t)$ and $v_{\mathrm{d1}}(t) = v_{\mathrm{d3}}(t)$. Since $\mathcal{E}\{2v_{\mathrm{d3}}(t)\} = -v_{\mathrm{out}}$, the operating point is calculated as $a = -\frac{v_{\mathrm{out}}}{2}$, and z_{dc} can be obtained for all the diodes as in (2). The choice of a affects the values of k_i', but the waveform optimization algorithm is only sensitive to k_2 and k_4 (and therefore not a) [3]. Consequently, the solution to the optimization problem and the design of low-complexity waveforms remain unchanged for multiple-diode rectennas.

Last but not least, it is important to note that while the optimized and proposed waveforms are adaptive to the CSI, the rectifiers as designed and simulated are not adaptive to the CSI. This is because the wireless channel changes in practice so quickly that it would be impractical for energy-constrained devices to dynamically compute and adjust the matching and the load as a function of the channel. This channel-adaptive signal approach makes the transmitter smarter and decreases the need for power-hungry optimization at the devices.

The prototyping and experimentation of the channel-adaptive waveforms are clearly beyond the scope of this letter. It would require the implementation of a closed-loop WPT architecture with a real-time over-the-air transmission based on a frame structure switching between a channel acquisition phase and WPT phase. The channel acquisition needs to be done at the millisecond level (similarly to CSI acquisition in communication). Different blocks need to be built, namely channel estimation, waveform design, and rectenna (including losses due to substrate, layout parasitics, and matching network). For preliminary results on the prototyping and experimentation of such an architecture making use of the SMF waveform, the readers are referred to [12].

V. Conclusion

This letter derives a methodology to design low-complexity adaptive waveforms for WPT. Assuming the CSI is available to the transmitter, the waveforms are designed such that more (resp. less) power is allocated to the frequency components corresponding to large (resp. weak) channel gains. They are shown through realistic simulations to achieve performance very close to the optimal waveforms in various rectenna configurations. Thanks to their low complexity, the proposed waveforms are very suitable for practical implementation.

References

[1] H. J. Visser and R. J. M. Vullers, "RF energy harvesting and transport for wireless sensor network applications: Principles and requirements," *Proc. IEEE*, vol. 101, no. 6, pp. 1410–1423, Jun. 2013.

[2] Y. Zeng, B. Clerckx, and R. Zhang, "Communications and signals design for wireless power transmission," *IEEE Trans. Commun.*, vol. 65, no. 5, pp. 2264–2290, May 2017.

[3] B. Clerckx and E. Bayguzina, "Waveform design for wireless power transfer," *IEEE Trans. Signal Process.*, vol. 64, no. 23, pp. 6313–6328, Dec. 2016.

[4] M. S. Trotter, J. D. Griffin, and G. D. Durgin, "Power-optimized waveforms for improving the range and reliability of RFID systems," in *Proc. 2009 IEEE Conf. RFID*, pp. 80–87.

[5] A. Boaventura, A. Collado, N. B. Carvalho, and A. Georgiadis, "Optimum behavior: Wireless power transmission system design through behavioral models and efficient synthesis techniques," *IEEE Microw. Mag.*, vol. 14, no. 2, pp. 26–35, Mar. 2013.

[6] C. R. Valenta, M. M. Morys, and G. D. Durgin, "Theoretical energy-conversion efficiency for energy-harvesting circuits under power-optimized waveform excitation," *IEEE Trans. Microw. Theory Techn.*, vol. 63, no. 5, pp. 1758–1767, May 2015.

[7] F. Bolos, Javier Blanco, A. Collado, and A. Georgiadis, "RF energy harvesting from multi-tone and digitally modulated signals," *IEEE Trans. Microw. Theory Techn.*, vol. 64, no. 6, pp. 1918–1927, Jun. 2016.

[8] B. Clerckx, E. Bayguzina, D. Yates, and P. D. Mitcheson, "Waveform optimization for wireless power transfer with nonlinear energy harvester modeling," in *Proc. IEEE Int. Symp. Wireless Commun. Syst.*, 2015, pp. 276–280.

[9] Y. Huang and B. Clerckx, in *Proc. 17th IEEE Int. Workshop Signal Process. Adv. Wireless Commun.*, 2016, pp. 1–5.

[10] M. Chiang, "Geometric programming for communication systems," *Found. Trends Commun. Inf. Theory*, vol. 2, no. 1/2, pp. 1–154, 2005.

[11] J. Medbo and P. Schramm, "Channel models for HIPERLAN/2 in different indoor scenarios," 3ERI085B, ETSI EP BRAN, Mar. 1998.

[12] J. Kim, B. Clerckx, and P. D. Mitcheson, "Prototyping and experimentation of a closed-loop wireless power transmission with channel acquisition and waveform optimization," in *Proc. IEEE Wireless Power Trans. Conf.*, 2017, to be published.